

Elevation of plasma membrane permeability by laser irradiation of selectively bound nanoparticles

Cuiping Yao

Key Laboratory of Biomedical Information
Engineering of Ministry of Education
China
and
Xi'an Jiaotong University
Institute of Biomedical Engineering
School of Life Science and Technology
Xianning xi Road 28
Xi'an 710049, China
E-mail: yaocui ping@sohu.com

Ramtin Rahmzadeh

Research Center Borstel
Parkallee 1-40
D-23845 Borstel, Germany

Elmar Endl

University Bonn
Institute of Molecular Medicine and
Experimental Immunology
Sigmund Freud Strasse 25
D-53105 Bonn, Germany

Zhenxi Zhang

Key Laboratory of Biomedical Information
Engineering of Ministry of Education
China
and
Xi'an Jiaotong University
Institute of Biomedical Engineering
School of Life Science and Technology
Xianning xi Road 28
Xi'an 710049, China

Johannes Gerdes

Research Center Borstel
Parkallee 1-40
D-23845 Borstel, Germany

Gereon Hüttmann

University Lübeck
Institute of Biomedical Optics
Peter-Monnik-Weg 4
D-23562 Lübeck, Germany

1 Introduction

There are many situations in medicine and biology when it is desirable to introduce a macromolecule into the cytoplasm of mammalian cells. One important application is gene therapy, where it is necessary to deliver genes or synthetic oligonucle-

Abstract. Irradiation of nanoabsorbers with pico- and nanosecond laser pulses could result in thermal effects with a spatial confinement of less than 50 nm. Therefore absorbing nanoparticles could be used to create controlled cellular effects. We describe a combination of laser irradiation with nanoparticles, which changes the plasma membrane permeability. We demonstrate that the system enables molecules to penetrate impermeable cell membranes. Laser light at 532 nm is used to irradiate conjugates of colloidal gold, which are delivered by antibodies to the plasma membrane of the Hodgkin's disease cell line L428 and/or the human large-cell anaplastic lymphoma cell line Karpas 299. After irradiation, membrane permeability is evaluated by fluorescence microscopy and flow cytometry using propidium iodide (PI) and fluorescein isothiocyanate (FITC) dextran. The fraction of transiently permeabilized and then resealed cells is affected by the laser parameter, the gold concentration, and the membrane protein of the different cell lines to which the nanoparticles are bound. Furthermore, a dependence on particle size is found for these interactions in the different cell lines. The results suggest that after optimization, this method could be used for gene transfection and gene therapy. © 2005 Society of Photo-Optical Instrumentation Engineers. [DOI: 10.1117/1.2137321]

Keywords: laser; membrane permeabilization; transfection; micro- and nanoeffects; nanoparticles; antibody.

Paper 05029R received Feb. 3, 2005; revised manuscript received Aug. 8, 2005; accepted for publication Aug. 22, 2005; published online Dec. 8, 2005.

otides into the cell. A number of methods involving chemical, viral, or physical approaches have been developed to transfer DNA and other macromolecules into mammalian cells, although each method has limitations.¹ Also, the transfer of antibodies into cells has interesting applications such as the staining of intracellular structures in living cells.

With the constant progress in laser technology and laser applications many scientists turn their eyes to pulsed laser

Address all correspondence to Gereon Hüttmann, Institute of Biomedical Optics, University Lübeck, Peter-Monnik-Weg 4, D-23562 Lübeck, Germany. Tel: ++49-451-500-6530. Fax: ++49-451-5646. E-mail: huettmann@bmo.uni-luebeck.de

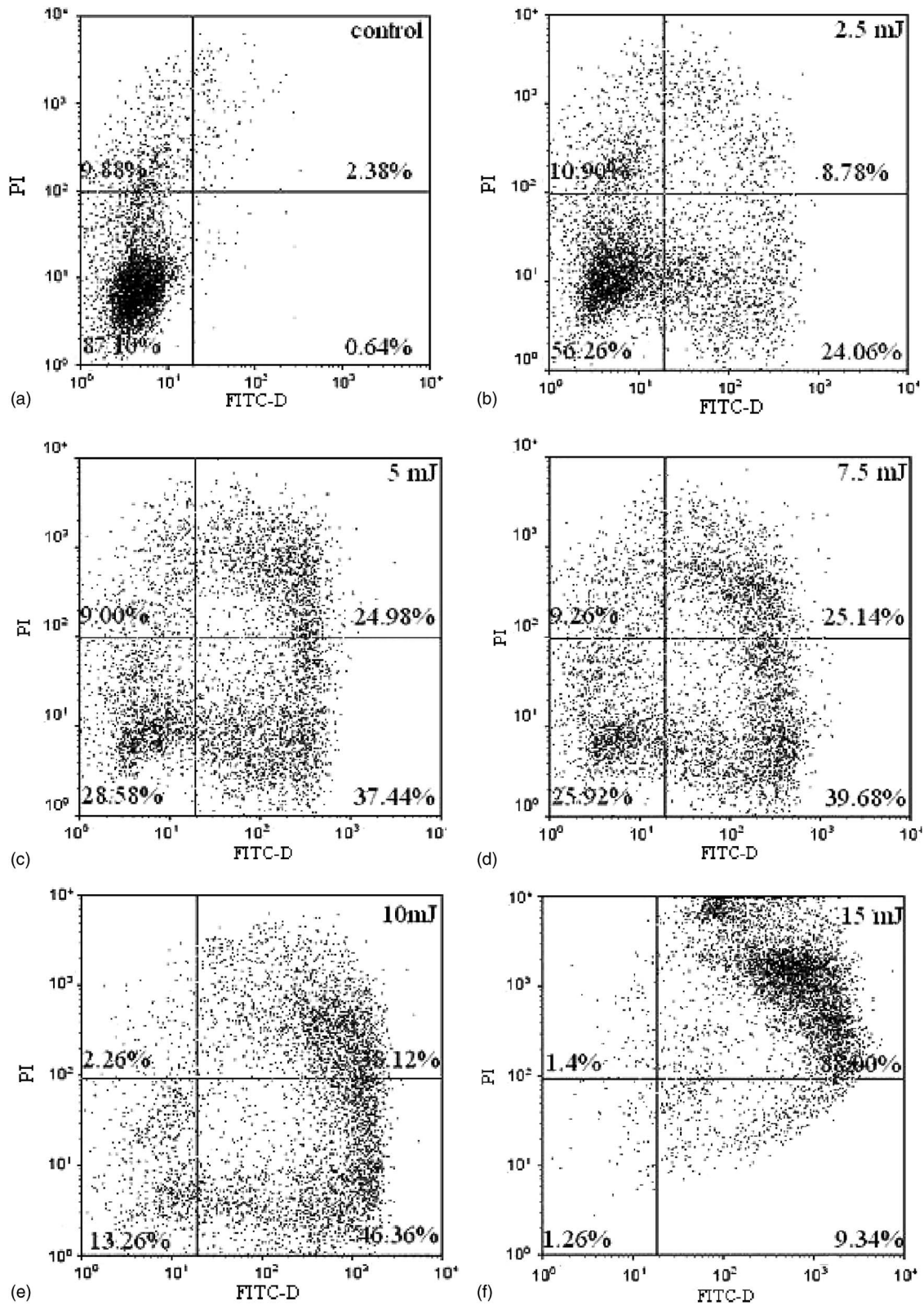


Fig. 1 Flow-cytometric measurements (scatter plots) of transient membrane permeabilization and cell death caused by laser-irradiated nanoparticles. Karpas 299 cells were incubated with 30-nm BerH2 gold conjugates. Nonirradiated cells served as control (a); samples were irradiated with different pulse energies: (b) 2.5, (c) 5, (d) 7.5, (e) 10, and (f) 15 mJ.

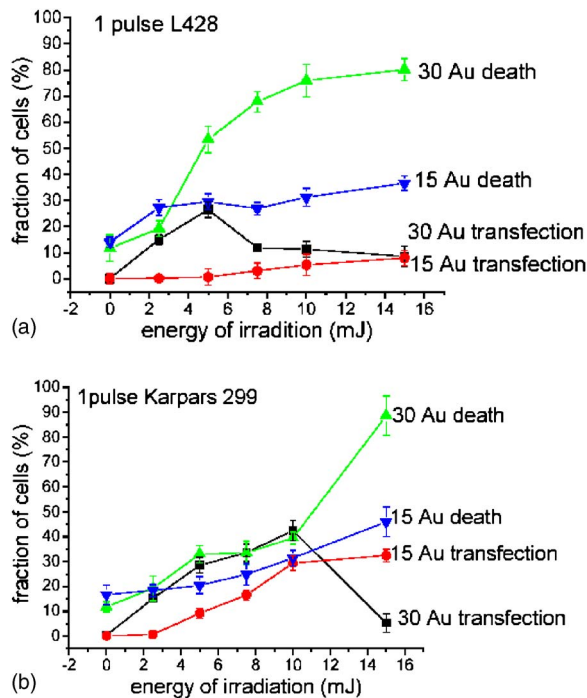


Fig. 2 Permeabilization efficiency and cell death of (a) L428 cell and (b) Karpas 299 cell after incubation with BerH2 gold particle conjugates of different diameters (15 and 30 nm). Cells were irradiated with a single pulse.

systems, using them for biotechnology. Currently three laser-based methods for gene transfer have been reported: microinjection, laser-induced stress waves, and selective cell targeting with light-absorbing particles. Microinjection was developed^{2,3} in the 1980s, but because this method uses focused microbeams that requires targeting each cell individually, this approach is both slow and limited to cell culture. It has not yet become a commonly used technique. There have been many reports on the application of laser-induced stress waves (LISWs) to drug delivery,⁴⁻⁷ but this method was capable of delivering only small drug molecules. Terakawa et al. recently reported the successfully delivery of plasmid DNA to mammalian cells by application of nanosecond pulsed laser-generated stress waves and an elevated temperature.⁸ Other studies have shown that laser-irradiated micro- and nanoparticles can selectively destroy cells or proteins.⁹⁻¹¹ Pitsillides et al.¹² and Umebayashi et al.¹³ reported an introduction of exogenous materials into the cytoplasm of living cells by irradiating gold nanoparticles or latex microparticles, respectively.

Gold nanoparticles, which are extensively used as immunoconjugates in electron microscopy, strongly absorb visible light. At their absorption peak around 520 nm, the absorption cross section can exceed the geometrical cross section, which enables an efficient heating of the particles by pulsed lasers to more than 1000 K. To achieve thermal confinement to a radius of less than 100 nm in water, the pulse duration should be⁹ shorter than 10 ns. Compared to microparticles, the smaller size of gold nanoparticles makes them more suitable for tissue-like samples or *in vivo* applications. Pitsillides et al.¹² were able to show the up-take of a 10-kDal dextran to T lymphocytes, which were isolated from fresh blood, with

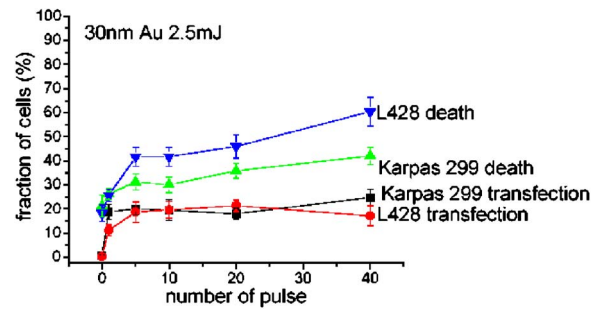


Fig. 3 Dependence of cell death and permeabilization efficacy on the number of applied pulses for 30-nm BerH2 conjugates for L428 and Karpas 299 cells. Samples were irradiated with 2.5 mJ.

20-nm particle diameter. However, slightly larger particles with 30-nm diameters either showed no effect or nearly complete cell killing. In that study, the experimental conditions were not varied in a systematic way and no numbers were given for the fraction of permeabilized cells. Additionally, rather long pulses that are commonly not available with *Q*-switched lasers were used. Therefore, the first report on nanoparticle-mediated cell permeabilization leaves open the question of how generally this method can be used to permeabilize cells and what efficacy can be achieved.

Based on that work, we systematically studied the ability of the nanoparticles to inflict the plasma membrane permeability without causing cell death in the two established cell lines L428 and Karpas 299 with different particle sizes, pulse energies, and particle densities. The L428 line is a long-term tissue culture line of Reed-Sternberg cells that was originally established from primary cells of a patient with Hodgkin's disease.¹⁴ The cells are positive for CD30, a member of the tumour necrosis factor receptor (TNFR) superfamily, which is found on Hodgkin/Reed-Sternberg (H/RS) cells, as well as on activated T and B lymphocytes. The human large-cell anaplastic lymphoma cell line Karpas 299 was established from blast cells in the peripheral blood of a 25-yr-old white man.¹⁵ Karpas 299 is positive for CD30 and CD25, which is the interleukin-2 receptor alpha chain. CD25 is expressed by early progenitors of T and B lineage as well as by activated mature T and B lymphocytes. The different structures of the both antigens might result in differing efficacies with which macromolecules are transferred into the cells. The degree of membrane permeabilization and the viability of cells were determined by flow cytometry, which measured the uptake of a fluorescing 10-kDal dextran (FITC-D) and propidium iodide (PI) to test permeabilization and cell death, respectively.

2 Materials and Methods

2.1 Apparatus

For all experiments sample irradiation was performed with a *Q*-switched frequency doubled Nd:YAG laser (Surelite I, Continuum, California, USA), which generates 6-ns pulses at 532 nm, in wells with a diameter of 2 mm, which were custom-made in a 25 × 75-mm slide of optical glass (Hellma). Each of the 18 wells took a sample volume of 4.0 μ l. The laser gave stable output energy with 10% standard deviation and a bell-shaped intensity distribution. The

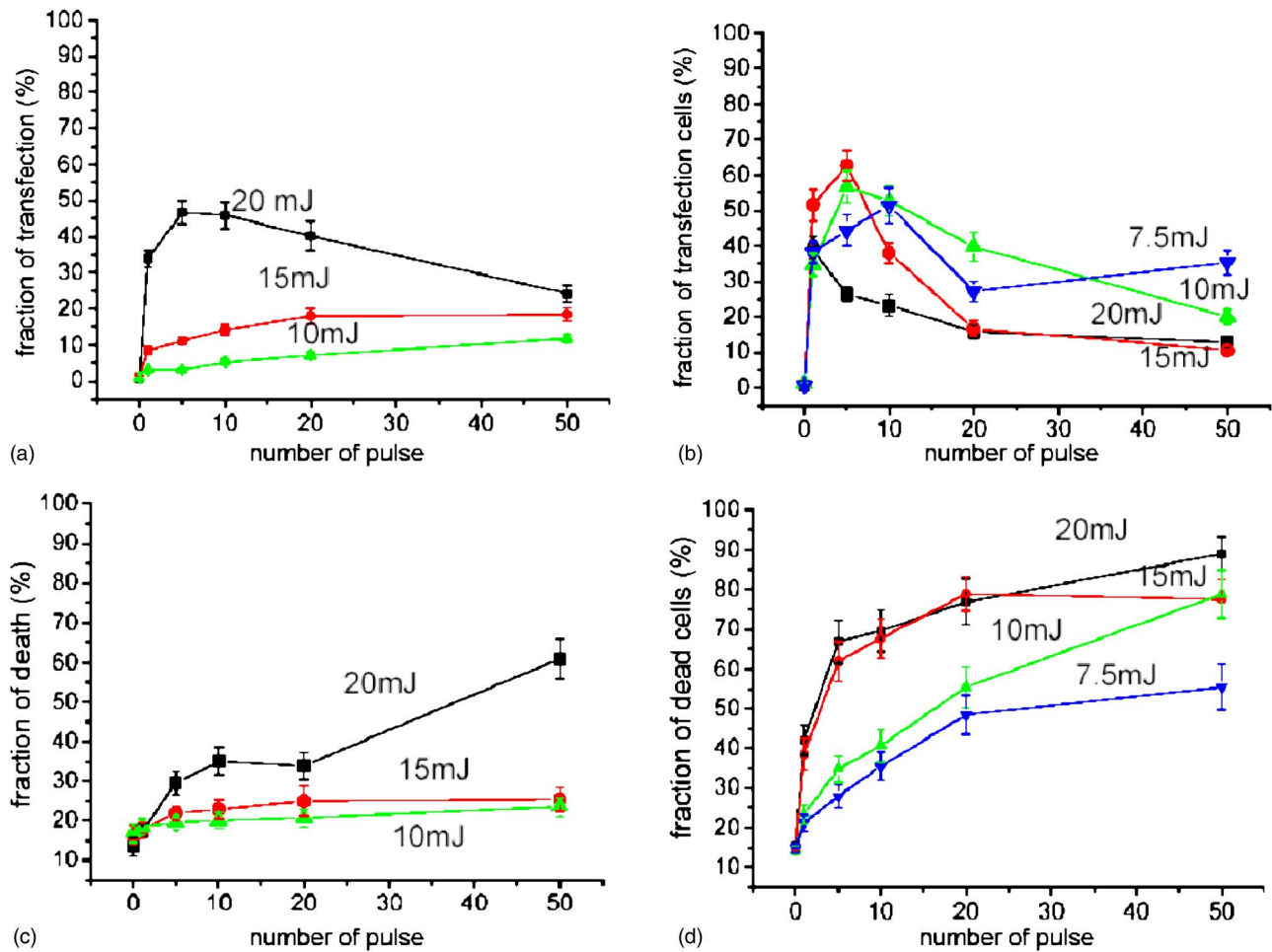


Fig. 4 Fraction of permeabilized cells [upper row, (a) and (b)] and dead cell [lower row, (c) and (d)]. Samples were irradiated with different energies and numbers of pulses. Karpas 299 cells were incubated with 15-nm ACT1 gold conjugates [left, (a) and (c)] and 30-nm ACT1 gold conjugates [right, (b) and (d)].

laser beam had a diameter of approximately 2 mm and the samples were irradiated with an unfocused beam. The radiant exposure in the center of the beam was 30 mJ/cm² for 1-mJ pulse energy and scaled linearly with the pulse energy. Either single pulses or multiple pulses at a frequency of 20 Hz were used.

Permeabilization of the plasma membrane and cell death were probed by fluorescence staining with FITC-D (molecular weight of 10,000 Dal, Molecular Probes) or PI, respectively. Fluorescence was quantified by a flow cytometer (FACSCAN, Beckman Coulter), in which the fluorescence of PI and FITC-D was excited by an argon ion laser emitting at 488 nm. Green fluorescence (for FITC-D) and red fluorescence (for PI) were collected using 525±5 nm bandpass and 600±5 nm longpass filters, respectively. Fluorescence data were stored and processed with WinMDI 2.8 software. A total of 5000 cells were examined in each sample. Results were confirmed by fluorescence microscopy (OLYMPUS BH2-RFL-T2), and the fluorescence images were recorded using a charge-coupled device (CCD) camera.

2.2 Cell Preparation

Hodgkin's disease cell line L428 and the human lymphoma cell line Karpas 299 were kindly provided by Prof. Horst

Dürkop, Institute for Pathology, Charité, Campus Benjamin Franklin, Berlin. Cells were routinely grown in suspension culture in a RPMI (Roswell Park Memorial Institute) 1640 (1×) with HEPES and L-Glutamine medium supplemented with 10% fetal calf serum, antibiotic/antimycotic solution (all cell culture media PAA Laboratories, Pasching, Austria) in a 37 °C humidified incubator (5% CO₂, 95% air). Cells at logarithmic growth phase were spun down at 1400 rpm for 5 min at 20 °C and then resuspended in phosphate-buffered saline (PBS) with different cell densities (4×10⁷/ml and 2×10⁷/ml). Immunogold particles, which were made from colloidal gold with diameters of 15 and 30 nm (British Biocell International) and the antibodies BerH2 against CD30 (Ref. 16) and ACT1 against CD25 (Ref. 17), were then added to the cell suspension at certain ratios of gold nanoparticles to number of cells. The mixture of cells and particles was incubated for 20 min at 37 °C. Immediately prior to irradiation, 10-kDa FITC-D was added to test membrane permeabilization. The amount of gold bound to the cells was estimated by absorption measurements at 520 nm (Lambda 14, Perkin Elmer, Überlingen, Germany). The mixture of cells, nanoparticles, and FITC-D was then transferred to an 18-well slide. At least 30 min after irradiation, during which the 18-well slide

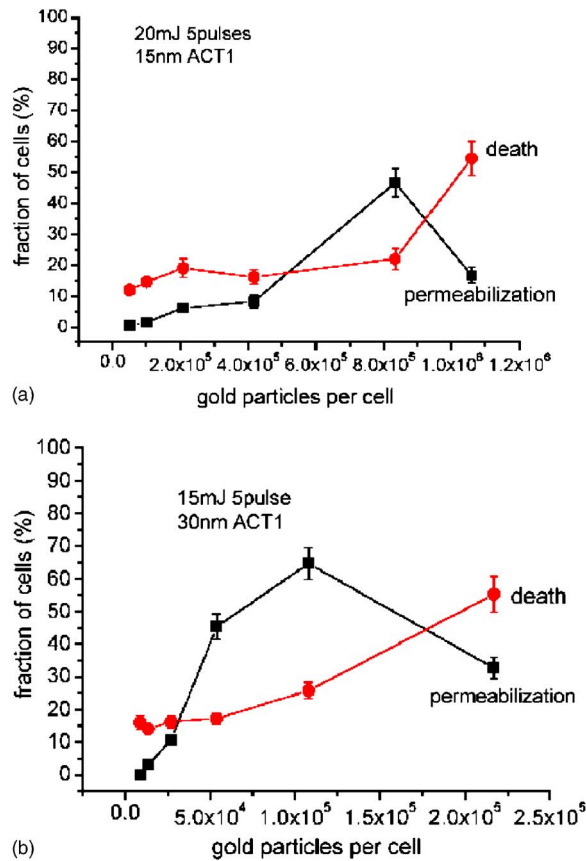


Fig. 5 Influence of ratios of gold conjugates on cells during incubation on membrane permeabilization and cell death for (a) 15- and (b) 30-nm ACT1 gold conjugates. Cells were irradiated with five pulses at 20 and 15 mJ pulse energies, respectively.

was kept in an incubator, the cells were washed with PBS and resuspended in PBS containing PI to assay cell death. Subsequently, the fluorescence of the cells was measured by flow cytometry.

3 Results

In this study, we used two cell lines (L428 and Karpas 299) and four different types of conjugates made from two different-sized gold nanoparticles (15 and 30 nm) and the two antibodies BerH2 and ACT1, which recognize CD30 and CD25 positive cells, respectively. Both cell lines were targeted by gold conjugate with the BerH2 antibodies. Additionally, ACT1 gold conjugates were used with Karpas 299 cells, which binds both antibodies. Therefore the influence of the cell type and the target receptor could be separated. Different numbers of pulses and pulse energies were used to find the optimal conditions for permeabilization of the plasma membrane. By comparing two different cell lines, the universality of this approach was confirmed.

3.1 Permeabilization of L428 and Karpas 299 with BerH2 Gold Conjugate

In the first experiment, single pulses were used and the influence of the pulse energy on permeabilization efficacy was tested in both cell lines with BerH2 conjugates. The cell den-

sity was 2×10^7 /ml. In the dot plot (Fig. 1) three subpopulations of the cells were seen as follows: intact viable cells exhibited no FITC-D and no PI fluorescence; transiently permeabilized cells containing only FITC-D but no PI; and permanently damaged or dead cells, which were positive for FITC-D and/or PI that was added at least 30 min after irradiation. Figure 1 shows the results for the Karpas 299 cell line with 30-nm BerH2 gold conjugates. From the dot plots, the fluorescence thresholds for FITC-D were chosen in such a way that in the control experiment less than 5% were positive for FITC-D. The threshold for the PI fluorescence lay half between the average fluorescence of viable and damaged cells. With these thresholds, the fractions of permeabilized and dead cells were calculated as shown in Fig. 2 for different pulse energies. Both the fraction of transiently permeabilized cells (lower right square) and damaged or dead cells (upper right square) increased with pulse energy. As expected from the lower absorption and the stronger effect of heat diffusion, 15-nm particles required more energy than 30-nm particles for permeabilization or cell killing.

The effect of multiple pulses was measured with 30-nm conjugates at single pulse energy of 2.5 mJ (Fig. 3). No significant dependence on the number of applied pulses was found when more than five pulses were applied. FITC-D and PI fluorescence increased with the number of pulses only for the range of one to five pulses.

3.2 Permeabilization of Karpas 299 Cell with ACT1 Gold Conjugates

Because Karpas 299 cells were easier to permeabilize and could be targeted by both antibodies, further experiments concentrated on this cell line. To determine the optimal conditions for the transfer of FITC-D into the cells, energy and pulse numbers were changed simultaneously. The cell density was 4×10^7 /ml, and the ratio of gold particles to cells remained unchanged. The results are shown for 15- and 30-nm particles in Fig. 4.

Both the number of permeabilized cells and dead cells first increased with the pulse energy and number of applied pulses. More permeabilized than dead cells were observed at appropriate conditions. When the energy and the number of the pulses exceeded a certain value, the fraction of permeabilized cells decreased and the fraction of dead cells increased strongly. The 30-nm particles were more efficient for permeabilization than the 15-nm particles, which was in agreement with the experiments using BerH2 immunogold particles.

3.3 Influence of the Ratio of the Gold Concentration During Incubation on the Membrane Permeabilization

To investigate the effect of the numbers of particles bound to the cells on the transient cell membrane permeabilization, we used different concentrations of particles and cells during the incubation. With an increased ratio of particles to cells, the percentage of dead cells increased, whereas the fraction of successfully permeabilized and resealed cells depended on the gold concentration in a form that resembled a normal distribution (Fig. 5).

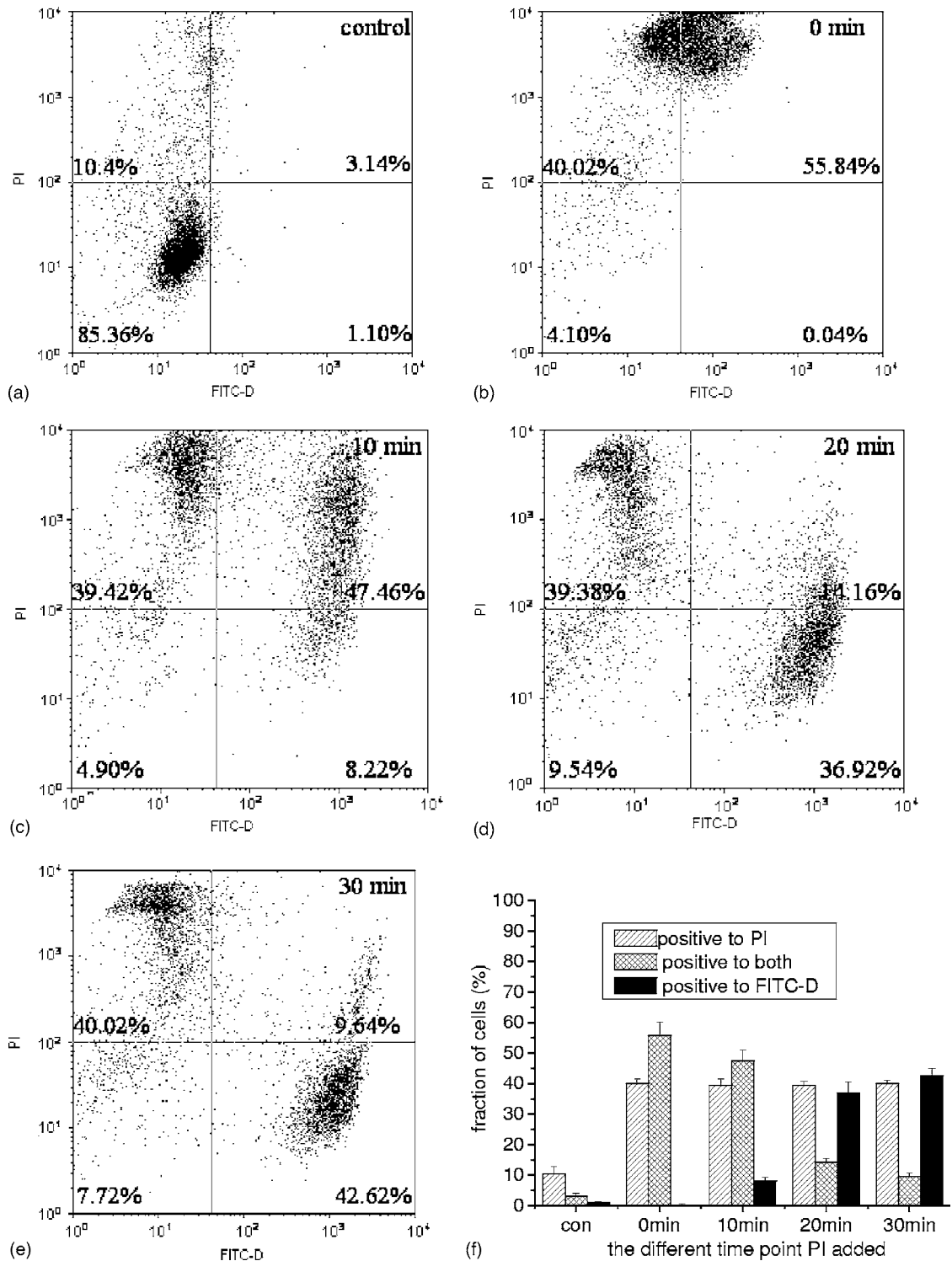


Fig. 6 Uptake of PI when added at different times after irradiation. Karpas 299 cells were incubated with 30-nm BerH2 gold conjugates and irradiated with 10 mJ and five pulses. PI was added (b) directly after irradiation, (c) after 10 min, (d) after 20 min, and (e) after 30 min. Control measurements are shown in (a). (f) The fraction of PI-positive and FITC-D-positive cells.

3.4 Time for the Resealing of the Cell Membrane

To study the time at which the cell membrane reseals, Karpas 299 cells were irradiated and the PI was added at different times after the irradiation (Fig. 6). As expected, nearly all cells are PI positive when this comparatively small molecule

is added directly after irradiation. As the time at which PI was added was increased, the fraction of PI-positive cells decreased and the number of FITC-positive cells increased. After 30 min, the cell membrane was completely closed for PI uptake.

Table 1 The best efficacies for the transfer of 10 kDal FITC-D into Karpas 299 and L428 cells with the corresponding irradiation parameters.

Cell Lines	Particles	BerH2 30 nm	BerH2 15 nm	ACT1 30 nm	ACT1 15 nm
Karpas 299	Transfection efficiency	42%	32%	68%	47%
	Irradiation parameters	10 mJ 1 pulse	15 mJ 1 pulse	15 mJ 5 pulses	20 mJ 5 pulses
	Particle load	2.5×10^4 /cell	5.9×10^5 /cell	1.1×10^5 /cell	8.3×10^5 /cell
L428	Transfection efficiency	26%	8%		
	Irradiation parameters	5 mJ 1 pulse	15 mJ 1 pulse		
	Particle load	1.4×10^4 /cell	2.4×10^5 /cell		

4 Conclusion and Discussion

The presented study shows that the combination of gold-antibody conjugate, which binds to the cell membrane, with laser light irradiation can be used to increase the membrane permeability. A 10-kDal molecule, which normally does not cross the cell membrane, can be transferred into the cells. This study with two cell lines investigated the effects of different energy levels, numbers of laser pulses, particle diameters, and cell:particle ratios on transient plasma membrane permeabilization to determine optimal conditions (Table 1).

In both cell lines and with both particle diameters, a transfer of FITC-D into the cells was possible. Efficiencies of more than 26% were reached for all combinations at optimized irradiation parameters, except for 15-nm nanoparticles and L428 cells. An increase of pulse energy, number of pulses, or loading of the cells with gold particles beyond the optimal parameters invariably caused cell death. Small particles required higher pulse energies due to smaller absorption and higher loss of energy by heat conduction during the laser pulse. Permeabilization was easier with the Karpas 299 cell line than with the L428 cell line. Finally, experiments with ACT1-gold conjugate provided better results. In contrast to Pitsillides et al.,¹² who were not able to use 30-nm particles successfully, we showed that both 30 and 15-nm gold particles could achieve membrane permeabilization, and the 30-nm particle even gave better results. Under optimal conditions 68% of the cells were loaded with FITC-D. Therefore, we conclude that no dramatic dependence on particle size exists when experimental conditions are adjusted correctly.

From a synopsis of all our experimental results, we conclude that permeabilization by the nanoparticle system is connected with an increase of cell death. Deviation from the optimal pulse energy or particle concentration by 50% reduces the transfer efficacy for FITC-D significantly and damages the cells to a large extent. Permeabilization seems to be a subtle effect of the nanoparticles on the cells and a careful optimization of all parameter seems to be necessary.

Beside the different cell system and the three times longer pulse width, the deviations of these results from the work of Pitsillides et al.¹² could also be caused by aggregation of gold particles and the temporal structure of the laser pulses, which both influence the reproducibility of the experiments. Aggregation of particle effectively enlarges the particle size, which increases the biological effect of the particles, as can be seen from our experiments with 15- and 30-nm-sized particles and

from temperature calculations.¹⁸ Aggregation may have occurred when the antibodies were conjugated to the particles, although we tried our best to optimize the protocols. It may also result because of a nonisotropic distribution of the receptors to which the particles bind on the cell surface. Due to the statistical interference of the longitudinal modes in the *Q*-switched Nd:YAG laser, which was used for irradiation, the laser pulse consists of a series of very short spikes, which change in a statistical fashion. This effect is common to all *Q*-switched lasers that are not single longitudinal mode. The spikes cause statistical temperature variation on the surface of the gold particles, which may to influence our results, especially with single pulses.

There are three possible reasons for the disparity in ACT1 or BerH2 gold conjugate performances. First, the number of particles bound to the cells is different. The amount of the antigen CD30 on the Karpas 299^{19,20} is as almost twice that on the L428, which was confirmed by absorption measurements. Second, different distribution of the receptors on the cell surface, and finally, a difference in structure of the receptor (CD25 and CD30) or position of binding site of the antibody²¹ could be responsible.

The mechanisms of the nanoparticle-based techniques for cell permeabilization is still unclear. In any case, a high local temperature is created in and around the particles during membrane permeabilization. Estimates of the temperatures^{11,12,18} for our experimental conditions give a temperature increase of 900 K when 15-nm particles are irradiated with 10 mJ. The 30-nm particles are heated to 3600 K. These temperatures are high enough to evaporate water in a layer around the particles, which creates a rapidly expanding bubble. Such bubbles with submicrometer diameters around gold nanoparticles were experimentally observed under laser irradiation.^{22,23} Additionally, the gold melts^{24,25} and breaks up into smaller particles. Particle fragmentation was observed at a radiant exposure starting from 80 mJ/cm² for 40-nm particles.^{26,27} Since under nanosecond irradiation the particle temperature scales with the square of the particle diameter, at fixed radiant exposure, the melting temperature will not be reached for particles below a certain diameter. Therefore, after a certain number of pulses, no further effect is expected when all particles are fragmented. This effect explains the comparably weak dependence of permeabilization and cell death on the number of pulses. Cavitation bubbles were also proposed by Pitsillides et al. as the mechanism for

cellular effects caused by laser-irradiated nanoparticles.¹² Although bubble formation does certainly occur under our irradiation conditions and the spatial extend of the bubbles²³ is expected to be larger than the volume that is directly heated by the particle,¹² we cannot rule out the possibility that a direct damage to the targeted protein also contributes to membrane permeabilization or cell killing.

The effects of laser-irradiated gold particles on the cell membranes seem to be more drastically than in the laser induced stress waves (LSWs) experiment. Membrane permeabilization caused by LSWs recovered completely²⁸ within 80 s after LSW. With nanoparticles, the permeabilization for PI persisted up 30 min after light irradiation (Fig. 6). Therefore the mechanism involved in the permeabilization and recovery of the plasma membrane caused by LSW may be different from those involved in our experiment. One advantage of the current approach over LSW is that the effects of the irradiation are mainly localized to cells to which the particles are bound, thereby enabling a selective permeabilization.

In summary, this paper describes a technique that can be used to transfer relatively small exogenous molecules into cells. Immunogold particles were bound to membrane proteins and introduced into living cells by irradiation with nanosecond pulses transiently permeabilizing the plasma membranes for exogenous macromolecules. The described technique shows many advantages including high efficiency (68% permeabilized cells and 27% dead cells). Furthermore, our recent experiments show that larger molecules such as fluorescent antibodies can be transferred into L428 and Karpas 299 cells by this method, labeling internal structures. Future experiments are under way to improve the procedure for a transfer of antibodies and the transfection with genetic material.

Acknowledgments

We thank Heyke Diddens, Barbara Flucke, Margit Kernbach, and Astrid Rodewald for their help during experiments. This work is supported by the National Nature Science Foundation of China (Grant No. 60178034 and No. 60378018) and the German Ministry for Education and Research (13N8461).

References

- N.-S. Yang, "Gene transfer into mammalian somatic cells," *Crit. Rev. Biotechnol.* **12**, 335–356 (1992).
- S. Kurata and Y. Ikawa, "Novel method for substance injection into the cell by laser beam—a study of the injection volume," *Cell Struct. Funct.* **11**, 205–207 (1986).
- S. Kurata, M. Tsukakoshi, T. Kasuya, and Y. Ikawa, "The laser method for efficient introduction of foreign DNA into cultured cells," *Exp. Cell Res.* **162**, 372–378 (1986).
- T. Kodama, M. R. Hamblin, and A. G. Doukas, "Cytoplasmic molecular delivery with shock waves: importance of impulse," *Biophys. J.* **79**, 1821–1832 (2000).
- G. Jagadeesh, K. Takayama, A. Takahashi, J. Kawagishi, J. Cole, and K. P. J. Reddy, "Micro-particle delivery using laser ablation," in *Proc. 23rd Int. Symp. on Shock Waves*, 785–788 (2001).
- M. Ogura, S. Sato, M. Kuroki, H. Wakisaka, S. Kawauchi, M. Ishihara, M. Kikuchi, M. Yoshioka, H. Ashida, and M. Obara, "Transdermal delivery of photosensitizer by the laser-induced stress wave in combination with skin heating," *Jpn. J. Appl. Phys., Part 2* **41**, L814–L816 (2002).
- T. Kodama, A. G. Doukas, and M. R. Hamblin, "Delivery of ribosome-inactivating protein toxin into cancer cells with shock waves," *Cancer Lett.* **189**, 69–75 (2003).
- M. Terakawa, M. Ogura, S. Sato, H. Wakisaka, H. Ashida, M. Uenoyama, Y. Masaki, and M. Obara, "Gene transfer into mammalian cells by use of a nanosecond pulsed laser-induced stress wave," *Opt. Lett.* **29**, 1227–1229 (2004).
- R. R. Anderson and J. A. Parrish, "Selective photothermolysis: Precise microsurgery by selective absorption of pulsed radiation," *Science* **220**, 524–527 (1983).
- D. Leszczynski, C. M. Pitsillides, R. K. Pastila, R. R. Anderson, and C. P. Lin, "Laser-beam-triggered microcavitation: a novel method for selective cell destruction," *Radiat. Res.* **156**, 399–407 (2001).
- G. Huettmann, J. Serbin, B. Radt, B. I. Lange, and R. Birngruber, "Model system for investigating laser-induced subcellular microeffects," *Proc. SPIE* **4257**, 398–409 (2001).
- C. M. Pitsillides, E. K. Joe, X. Wei, R. R. Anderson, and C. P. Lin, "Selective cell targeting with light-absorbing microparticles and nanoparticles," *Biophys. J.* **84**, 4023–4032 (2003).
- Y. Umebayashi, Y. Miyamoto, M. Wakita, A. Kobayashi, and T. Nishisaka, "Elevation of plasma membrane permeability on laser irradiation of extracellular latex particles," *J. Biochem. (Tokyo)* **134**, 219–224 (2003).
- M. Schaadt, V. Diehl, H. Stein, C. Fonatsch, and H. H. Kirchner, "Two neoplastic cell lines with unique features derived from Hodgkin's disease," *Int. J. Cancer* **26**, 723–731 (1980).
- P. Fischer, E. Nacheva, D. Y. Mason, P. D. Sherrington, C. Hoyle, F. G. Hayhoe, and A. Karpas, "A Ki-1 (CD30)-positive human cell line (Karpas 299) established from a high-grade non-Hodgkin's lymphoma, showing a 2;5 translocation and rearrangement of the T-cell receptor beta-chain gene," *Blood* **72**, 234–240 (1988).
- R. Schwarting, J. Gerdes, H. Durkop, B. Falini, S. Pileri, and H. Stein, "Ber-H2: a new anti Ki-1 (CD30) monoclonal antibody directed at a formol-resistant epitope," *Blood* **74**, 1678–1689 (1989).
- R. Schwarting, J. Gerdes, J. A. Ziegler, and H. Stein, "Immunoprecipitation of the interleukin-2 receptor from Hodgkin's disease derived cell lines by monoclonal antibodies," *Hematol. Oncol.* **5**, 57–64 (1987).
- G. Huettmann and R. Birngruber, "On the possibility of high-precision photothermal microeffects and the measurement of fast thermal denaturation of proteins," *IEEE J. Sel. Top. Quantum Electron.* **5**, 954–962 (1999).
- A. F. Wahl, K. Klussman, J. D. Thompson, J. H. Chen, L. V. Francisc, G. Risdon, D. F. Chace, C. B. Siegall, and J. A. Francisco, "The Anti-CD30 monoclonal antibody SGN-30 promotes growth arrest and DNA fragmentation *in vitro* and affects antitumor activity in models of Hodgkin's disease," *Cancer Res.* **62**, 3736–3742 (2002).
- H. J. Gruss, N. Boiani, D. E. Williams, R. J. Armitage, C. A. Smith, and R. G. Goodwin, "Pleiotropic effects of the CD30 ligand on CD30-expressing cells and lymphoma cell lines," *Blood* **83**, 2045–2056 (1994).
- L. Dong, M. Huelsmeyer, H. Durkop, H. P. Hansen, J. Schneider-Mergener, A. Ziegler, and B. Uchanska-Ziegler, "Human CD30: structural implications from epitope mapping and modelling studies," *J. Mol. Recognit.* **16**, 28–36 (2003).
- V. P. Zharov and V. Galitovsky, "Photothermal detection of local thermal effects during selective nanophotothermolysis," *Appl. Phys. Lett.* **83**(24), 4897–4899 (2003).
- A. Plech, V. Kotaidis, M. Lorenc, and M. Wulff, "Thermal dynamics in laser excited metal nanoparticles," *Chem. Phys. Lett.* **401**, 565–569 (2005).
- S. Link, C. Burda, M. M. B. B. Nikoobakht, and M. A. El-Sayed, "Laser photothermal melting and fragmentation of gold nanorods: energy and laser pulse-width dependence," *J. Phys. Chem. A* **103**, 1165–1170 (1999).
- A. Plech, V. Kotaidis, S. Grésillon, C. Dahmen, and G. v. Plessen, "Laser-induced heating and melting of gold nanoparticles studied by time-resolved x-ray scattering," *Phys. Rev. B* **70**, 195423 (2004).
- H. Kurita, A. Takami, and S. Koda, "Size reduction of gold particles in aqueous solution by pulsed laser irradiation," *Appl. Phys. Lett.* **72**, 789–791 (1998).
- A. Takami, H. Kurita, and S. Koda, "Laser-induced size reduction of noble metal particles," *J. Phys. Chem. B* **103**, 1226–1232 (1999).
- S. Lee, T. Anderson, H. Zhang, T. J. Flotte, and A. G. Doukas, "Alteration of cell membrane by stress waves *in vitro*," *Ultrasound Med. Biol.* **22**(9), 1285–1293 (1996).